Supporting Information

C. Jake Harris*, Dylan Husmann*, Wanlu Liu, Farid El Kasmi, Haifeng Wang, Ashot Papikian, William A. Pastor, Guillaume Moissiard, Ajay A. Vashisht, Jeffery L. Dangl, James A. Wohlschlegel, Steven E. Jacobsen (2016)
Arabidopsis AtMORC4 and AtMORC7 Form Nuclear Bodies and Repress a Large Number of Protein-Coding Genes. PLoS Genet 12(5): e1005998. doi:10.1371/journal.pgen.1005998

S1 Fig. *atmorc4/7* double mutant shows de-repression at AtMORC6 transposon targets.
(A) RT-PCR on cDNA derived from *atmorc4-1/atmorc7-1* double mutant compared to wt showing no detectable wild type transcript in these T-DNA mutants. Primers were designed to span the T-DNA region in *atmorc4-1* (upper) and *atmorc7-1* (middle) (S1 Table). UBQ10 (lower) was amplified as a loading control (S1 Table). **(B)** RT-PCR at AtMORC6 targets indicated using the genotypes indicated. Error bars indicate standard error of the mean (SEM).
doi:10.1371/journal.pgen.1005998.s001
(PDF)

S2 Fig. *AtMORC3* is likely to be a pseudogene.
(A) TAIR predicted gene structure for *AtMORC1*, *AtMORC2*, and *AtMORC3*. Boxes = exons, light blue = UTR, and dark blue = CDS. *AtMORC1*, *AtMORC2*, and *AtMORC3* are highly related to one another, (see Fig 1A, and **(B)** below), encode the same number of exons, and lie directly adjacent to one another on *A*. *thaliana* chromosome four, indicating that they likely arose from a tandem duplication event. In the predicted 5' UTR of *AtMORC3*, there is an ATG start codon. However, a G to A mutation causes a W to Stop codon in exon three. BLAST of this *in silico* translated region identifies all other AtMORC proteins. However, because this ORF is predicted to be too small, TAIR finds the next in-frame ATG in exon 5, annotating this to be the translational start. If this protein were made, it would be N-terminally truncated, missing half of the GHKL ATPase including two out of the four motifs thought to be essential for ATP binding [28,29]. **(B)** Phylogenetic reconstruction of *AtMORC* genes in *Arabidopsis thaliana* and close relatives, *Capsella rubella* and *Arabidopsis lyrata*. The tandem arrangement of *AtMORC1*, *AtMORC2*, and *AtMORC3*, and the premature stop codon identified in *AtMORC3* is consistent with the pseudogenisation of a redundant paralogue. Therefore, we checked whether *AtMORC1*, *AtMORC2*, and *AtMORC3* are also present in *A*. *thaliana* sister species. We found that while the closely related *A*. *lyrata* encodes a single copy of each of *A*. *thaliana*'s *AtMORC* genes, the slightly more distantly related *C*. *rubella* does not encode a copy of either *AtMORC2* or *AtMORC3* (and encodes two copies of *AtMORC4*). Therefore *C*. *rubella* has either lost its versions of *AtMORC2*/*AtMORC3* or the tandem duplication of *AtMORC1* occurred after

the divergence of *A*. *thaliana* and *A*. *lyrata* from *C*. *rubella*. In either scenario, it suggests that *AtMORC2* and *AtMORC3* are likely non-essential and may act redundantly with *AtMORC1*. In support of this hypothesis, we have already shown that *AtMORC2* is redundant with *AtMORC1* [35]. **(C)** Positions of the SALK_000009 and SALK_043244 insertions in *AtMORC3*. **(D)** Sequence of SALK_043244 T-DNA homozygous insert in *AtMORC3*. As the SALK_000009 line, which has a T-DNA insert in the 5' UTR of *AtMORC3*, was found to be embryonic lethal [36], we took an independent *AtMORC3* T-DNA line to homozygosity and sequence confirmed the presence of the insert in exon 11, finding that this line displays no discernable phenotype. Together with the premature stop codon in exon 3, it is likely that *AtMORC3* is a non-functional pseudogene in Columbia-0.
doi:10.1371/journal.pgen.1005998.s002
(PDF)

S3 Fig. Comparison of RNA-seq in *atmorc4/6/7* vs. *atmorc1/2/4/5/6/7*.
(A) Overlap between *atmorc4/6/7* and *atmorc1/2/4/5/6/7* upregulated DEGs. **(B)** Boxplot showing the FPKM (fragments per kilobase per million reads) for the 241 genes in *atmorc1/2/4/5/6/7* that did not overlap with *atmorc4/6/7* (purple section in (**A**)). This shows that while these genes did not make the significance cutoff required to be called DEGs in *atmorc4/6/7*, they still show the same trend for upregulation, indicating that the addition of *atmorc1*, *2* and *5* has very little additional impact on the transcriptome (also see Fig 3D).
doi:10.1371/journal.pgen.1005998.s003
(PDF)

S4 Fig. DEGs in *atmorc4/7* are highly enriched for pathogen defense.
(A) Top ten listed GO term categories from *atmorc4/7* misregulated genes (FDR<0.05) [http://bioinfo.cau.edu.cn/agriGO] identified RNA-seq round 2 (see Fig 3). **(B)** Top ten listed GO term categories from *atmorc4/7* misregulated genes (FDR<0.05) [http://bioinfo.cau.edu.cn/agriGO] identified RNA-seq round 1 (see Fig 1).
doi:10.1371/journal.pgen.1005998.s004
(PDF)

S5 Fig. No additive transcriptional effect at 'response to chitin' genes in higher-order *atmorc* knockouts.
Boxplot showing FPKMs at the 'response to chitin' gene set (GO:0010200) in the genotypes indicated.
doi:10.1371/journal.pgen.1005998.s005
(PDF)

S6 Fig. Negligible DNA methylation changes genome wide and at AtMORC targets in *AtMORC* knockouts.
(A) Genome wide profiles of CG, CHG, and CHH context methylation in the wt, *atmorc4/7*, *atmorc6*, and *atmorc1/2/4/5/6/7* backgrounds. Average of two biological replicates of each genotype, except *atmorc6* (data obtained from GSE54677) [35]. **(B)** Metaplot of methylation levels in wt, *atmorc4/7* and *atmorc1/2/4/5/6/7* over DEGs (>2 fold change, FDR<0.05) in *atmorc1/2/4/5/6/7* background, in CG, CHG and CHH contexts. TSS =

transcriptional start site, TTS = transcriptional termination site.
doi:10.1371/journal.pgen.1005998.s006
(PDF)

S7 Fig. Loss of AtMORC does not significantly impact any of the major DNA methylation pathways and does not act downstream of DNA methylation.
(A) Boxplots for methylation levels at *drm1/2* CHH, *cmt2* CHH, *cmt3* CHG, and *met1* CG defined hypomethylated DMRs [8,49] in the wt, *atmorc4/7*, *atmorc6*, *atmorc1/2/4/5/6/7*, and control methyltransferase mutant backgrounds indicated. **(B)** RNA-seq from wt and *atmorc1/2/4/5/6/7* (black and green, respectively, three replicates each, see Fig 3) over methylated loci defined by *drm1/2* CHH, *cmt2* CHH, *cmt3* CHG, and *met1* CG hypo DMRs (as in (**A**)).
doi:10.1371/journal.pgen.1005998.s007
(PDF)

S8 Fig. *atmorc1/2/4/5/6/7* hypo CHH DMRs overlap with RdDM sites.
(A) Overlap of *atmorc1/2/4/5/6/7* defined hypo CHH DMRs with previously defined *drm1/2* and *cmt2* hypo CHH DMRs [8,49]. **(B)** Overlap of *atmorc1/2/4/5/6/7* hypo CHH DMRs with CHH loci prone to spontaneous epiallelic variation [50].
doi:10.1371/journal.pgen.1005998.s008
(PDF)

S9 Fig. Comparison of *atmorc6* with *atmorc4/7* at *atmorc1/2/4/5/6/7* hypo CHH DMRs.
(A) Heatmap showing CHH methylation levels at all *atmorc1/2/4/5/6/7* hypo CHH DMRs in the genotypes indicated. *atmorc4/7* and *atmorc6* appear to affect many similar targets. Scale 0–0.6 indicates CHH methylation level. (B) Boxplot for methylation levels at same *atmorc1/2/4/5/6/7* hypo CHH DMRs as in (A). *drm1/2* is used as a control in (A) and (B), and demonstrates that *atmorc* hypo CHH DMRs are primarily RdDM target loci.
doi:10.1371/journal.pgen.1005998.s009
(PDF)

S10 Fig. *atmorc1/2/4/5/6/7* hypo CHH DMRs show evidence for transcriptional de-repression.
(A) RNA-seq metaplot of wt vs. *atmorc1/2/4/5/6/7* (black and green, respectively, three replicates each, see Fig 3) over *atmorc1/2/4/5/6/7* defined hypo CHH DMRs. **(B)** RNA-seq metaplot of wt vs. *drm1/2* (black and red, respectively, two replicates each) over drm1/2 hypo CHH DMRs (data from GEO:GSE51304) [8].
doi:10.1371/journal.pgen.1005998.s010
(PDF)

S1 Video. AtMORC7-MYC rotate.
z-stack at 0.83 μM intervals through the AtMORC7-MYC expressing nucleus depicted in Fig 5A was rendered in 3D with interpolation and rotated 360 degrees about the *y*-axis. Blue channel = DAPI staining; green channel = anti-MYC staining.

doi:10.1371/journal.pgen.1005998.s011
(AVI)

S2 Video. AtMORC7-MYC stack.

z-stack at 0.83 μM intervals through the AtMORC7-MYC expressing nucleus depicted in Fig 5A. z-stack slices from the furthest to closest depth are shown in sequence (5 frames per second), illustrating the presence of AtMORC7-MYC bodies first at one chromocenter (upper middle of nucleolus) and then more prominently at another (middle left, between nucleolus and nuclear periphery). Blue channel = DAPI staining; green channel = anti MYC staining. Scale bar = 2 μM

doi:10.1371/journal.pgen.1005998.s012
(AVI)

S1 Table. Primers used in this study.

List of relevant primers used in the study.

doi:10.1371/journal.pgen.1005998.s013
(PDF)

Fig. S1: *atmorc4/7* double mutant shows de-repression at AtMORC6 transposon targets.

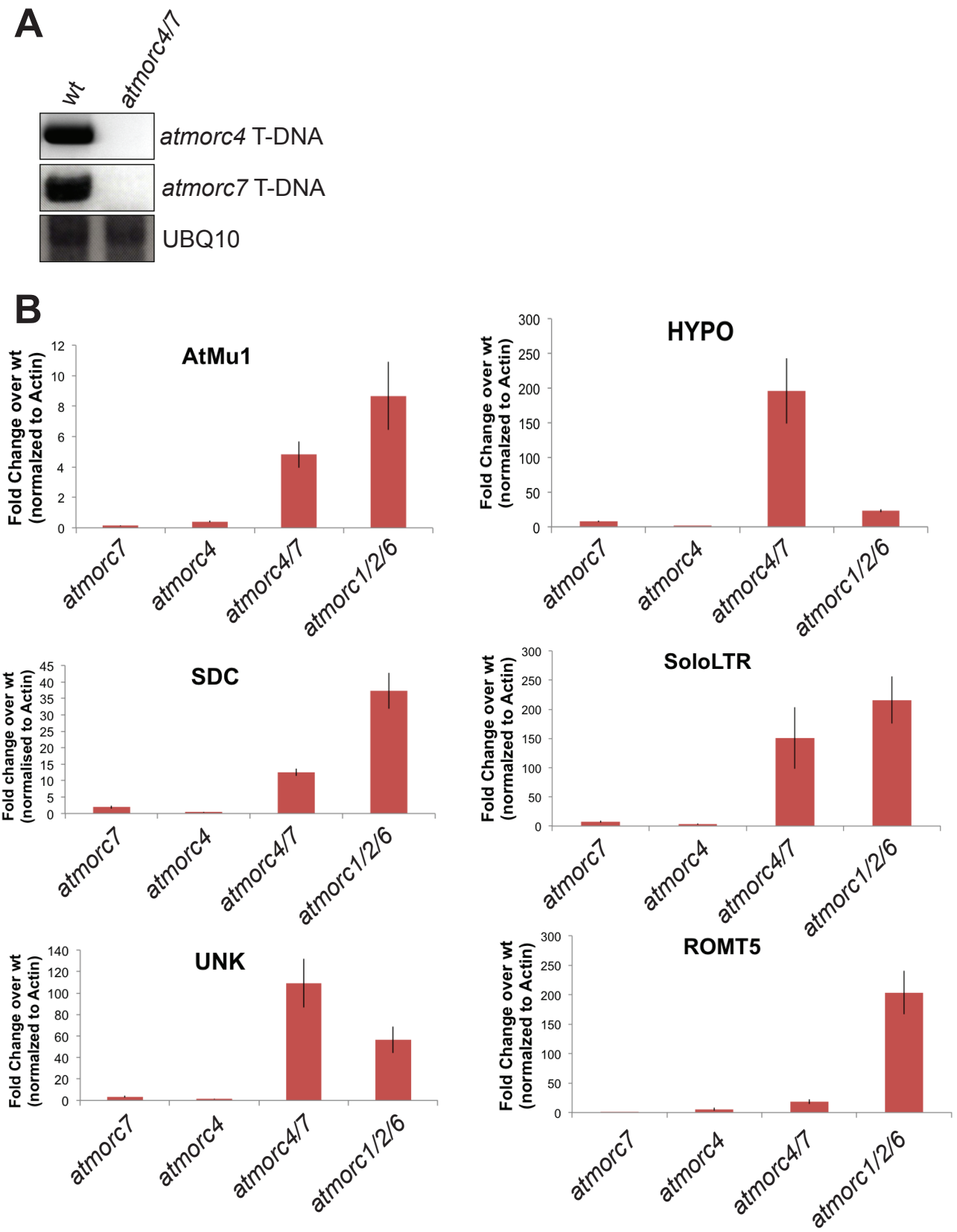

Fig. S2: *AtMORC3* is likely to be a pseudogene.

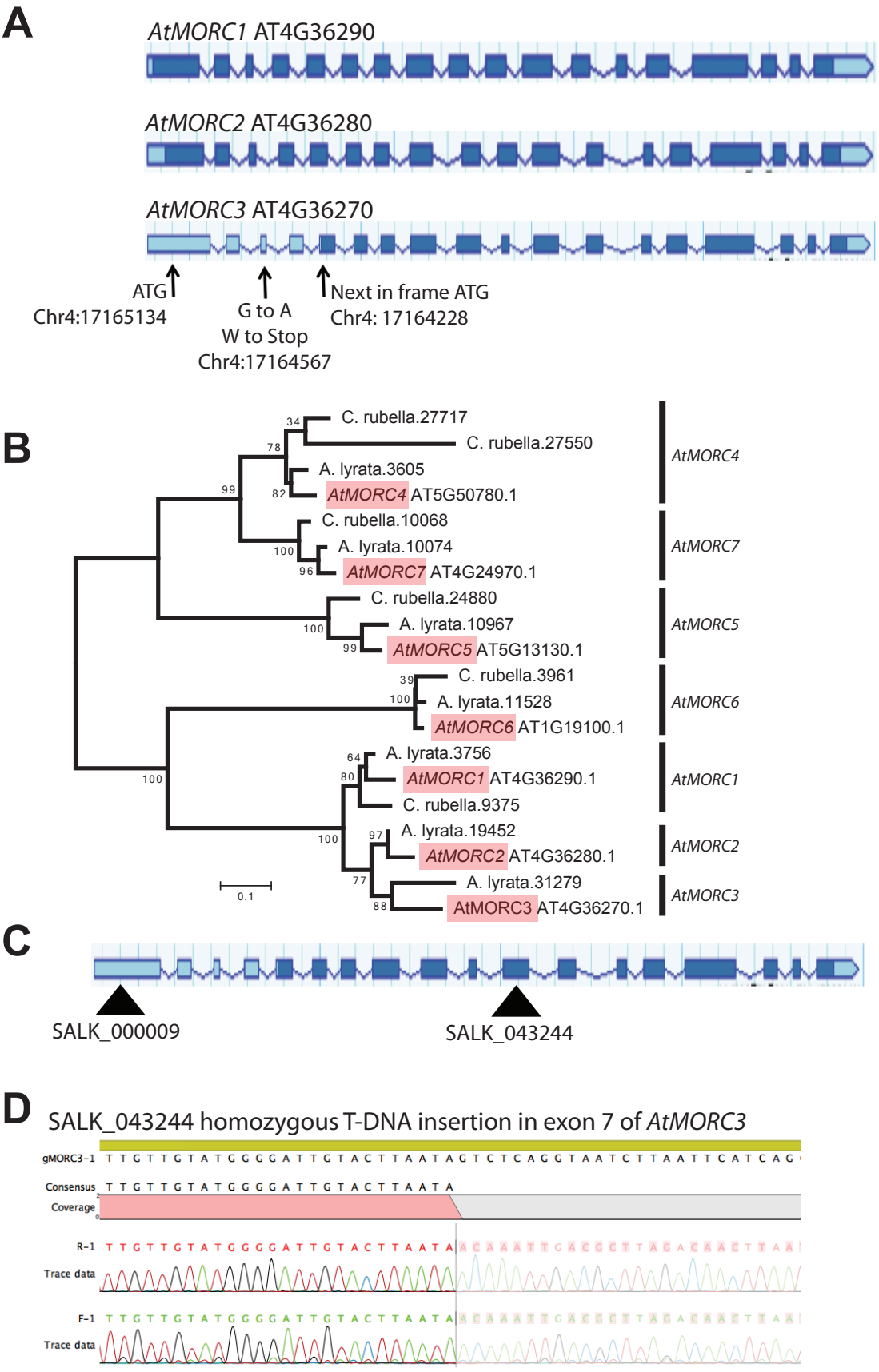

Fig. S3: Comparison of RNA-seq in *atmorc4/6/7* vs. *atmorc1/2/4/5/6/7*.

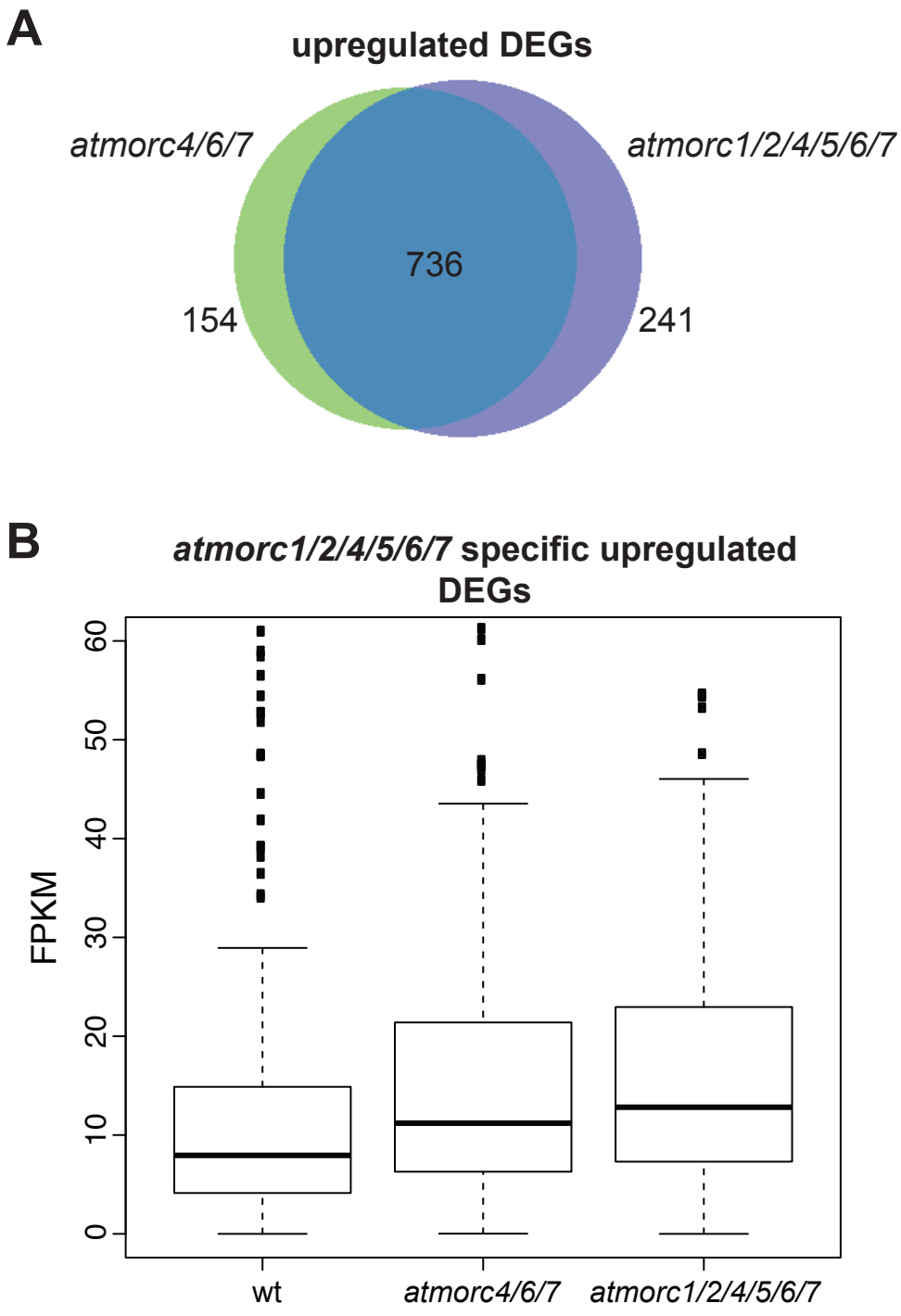

Fig. S4. DEGs in *atmorc4/7* are highly enriched for pathogen defense.

A

GO term	Ontology	Description	Number in input list	Number in BG/Ref	p-value	FDR
GO:0010200	P	response to chitin	57	151	4.2e-47	6.5e-44
GO:0009743	P	response to carbohydrate stimulus	63	240	5.8e-44	4.5e-41
GO:0050896	P	response to stimulus	229	4057	2.2e-43	1.1e-40
GO:0010033	P	response to organic substance	119	1342	5.1e-38	2e-35
GO:0042221	P	response to chemical stimulus	142	2085	1.1e-33	3.3e-31
GO:0006950	P	response to stress	138	2320	3.7e-27	9.5e-25
GO:0006952	P	defense response	66	766	1.2e-20	2.7e-18
GO:0002376	P	immune system process	43	368	3.6e-18	6.2e-16
GO:0006955	P	immune response	43	367	3.3e-18	6.2e-16
GO:0006468	P	protein amino acid phosphorylation	67	946	7.5e-17	1.2e-14

B

GO term	Ontology	Description	Number in input list	Number in BG/Ref	p-value	FDR
GO:0050896	P	response to stimulus	154	4057	1.1e-31	1.4e-28
GO:0042221	P	response to chemical stimulus	102	2085	2.4e-28	1.5e-25
GO:0010033	P	response to organic substance	79	1342	1.2e-26	5e-24
GO:0006950	P	response to stress	94	2320	1.5e-20	4.8e-18
GO:0009719	P	response to endogenous stimulus	61	1068	4.7e-20	1.2e-17
GO:0009725	P	response to hormone stimulus	55	982	8.3e-18	1.8e-15
GO:0010200	P	response to chitin	21	151	2.8e-14	5.2e-12
GO:0009743	P	response to carbohydrate stimulus	25	240	4.1e-14	6.6e-12
GO:0009611	P	response to wounding	21	197	3e-12	4.4e-10
GO:0009620	P	response to fungus	18	158	4e-11	5.2e-09

Fig. S5: No additive transcriptional effect at 'response to chitin' genes in higher-order *atmorc* knockouts.

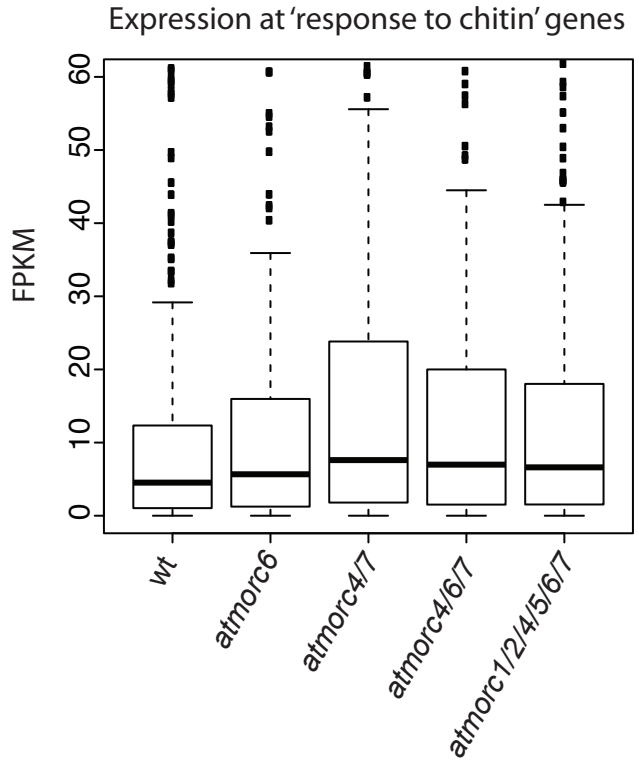

Fig. S6: Negligible DNA methylation changes genome wide and at AtMORC targets in *AtMORC* knockouts.

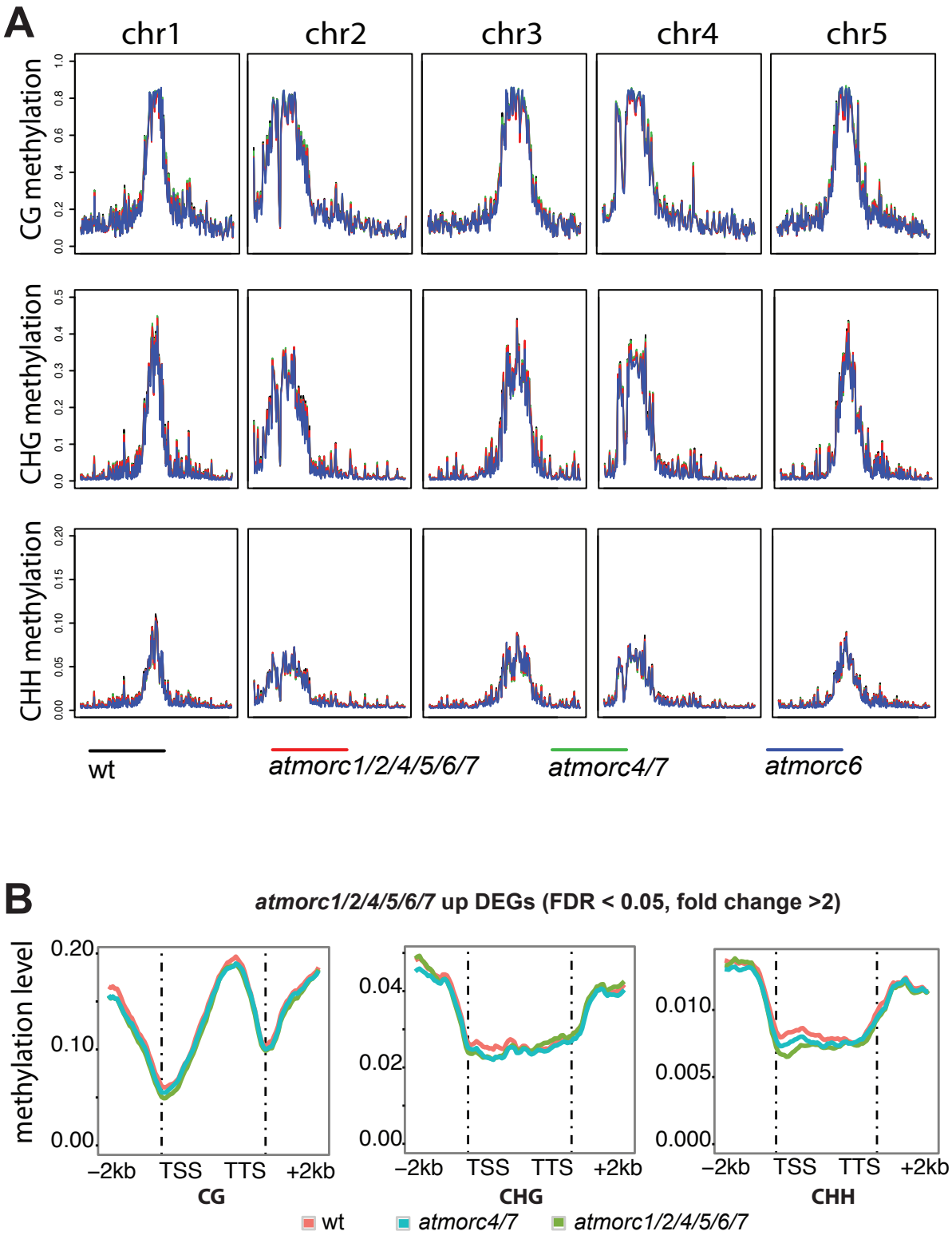

Fig. S7: Loss of AtMORC does not significantly impact any of the major DNA methylation pathways and does not act downstream of DNA methylation.

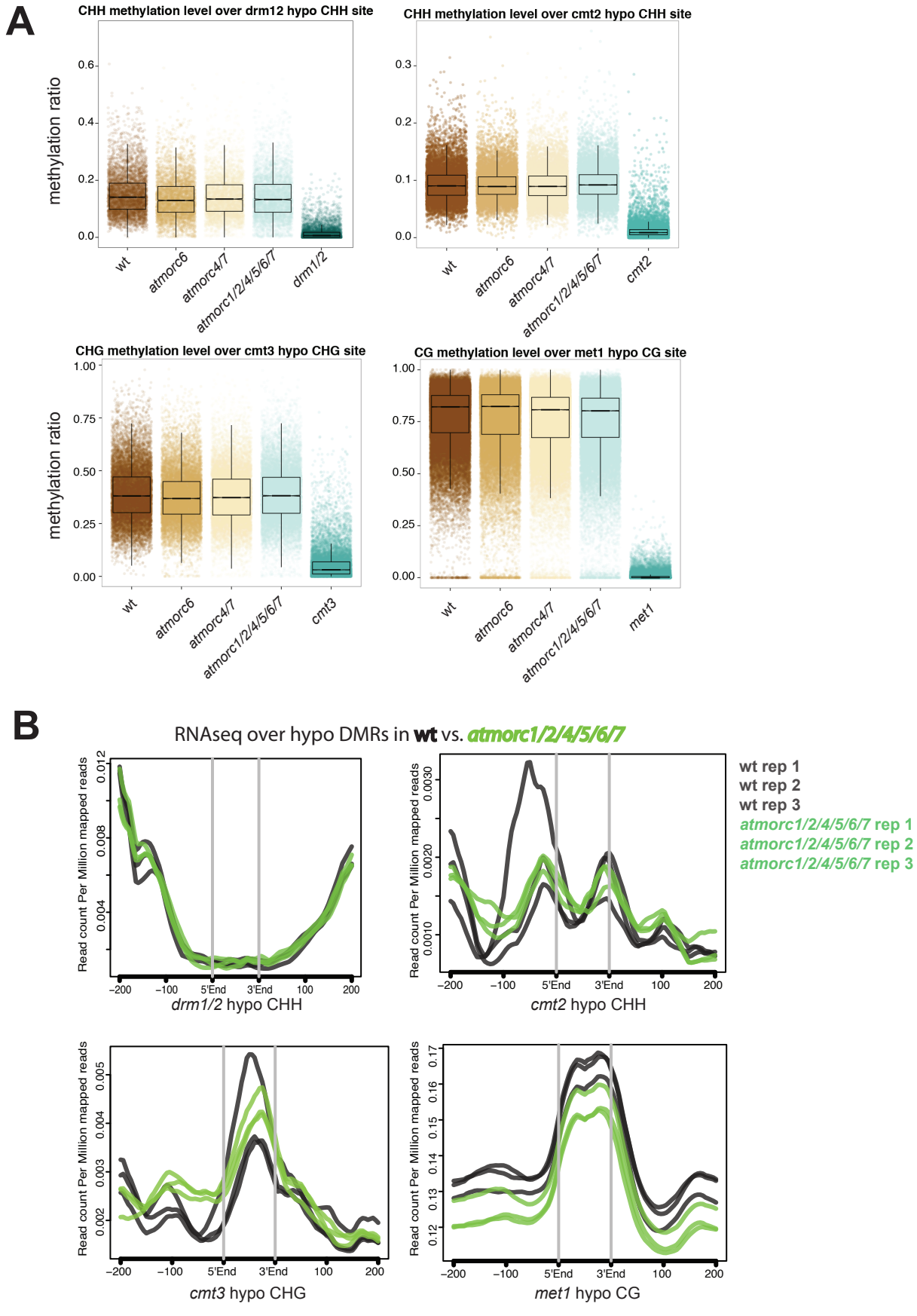

Fig. S8: *atmorc1/2/4/5/6/7* hypo CHH DMRs overlap with RdDM sites.

A

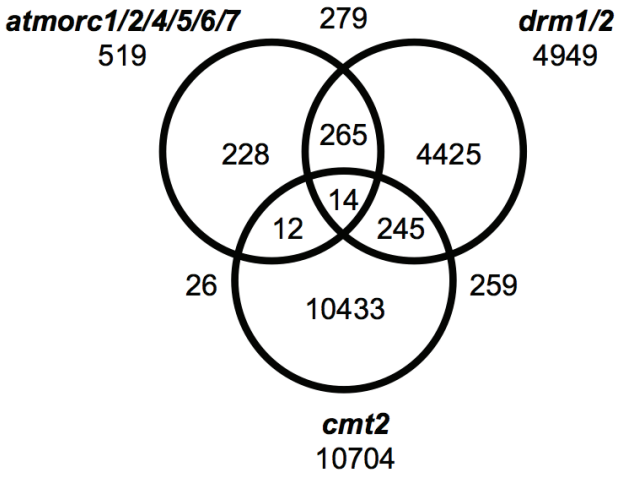

54% of *atmorc1/2/4/5/6/7* hypo CHH DMRs overlap with *drm1/2*
2% of *atmorc1/2/4/5/6/7* hypo CHH DMRs overlap exclusively with *cmt2*

B

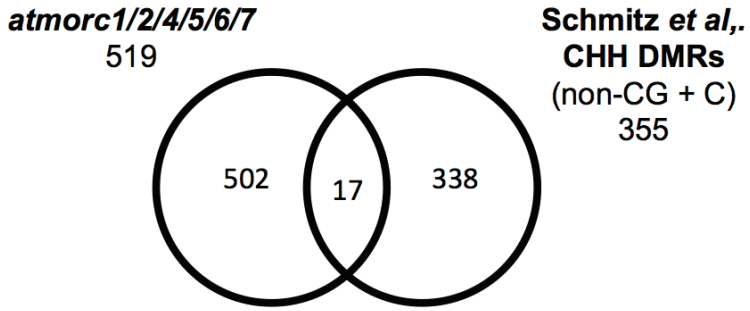

3% of *atmorc1/2/4/5/6/7* hypo CHH DMRs
overlap with spontaneous epi-alleles

Fig. S9: Comparison of *atmorc6* with *atmorc4/7* at atmorc1/2/4/5/6/7 hypo CHH DMRs.

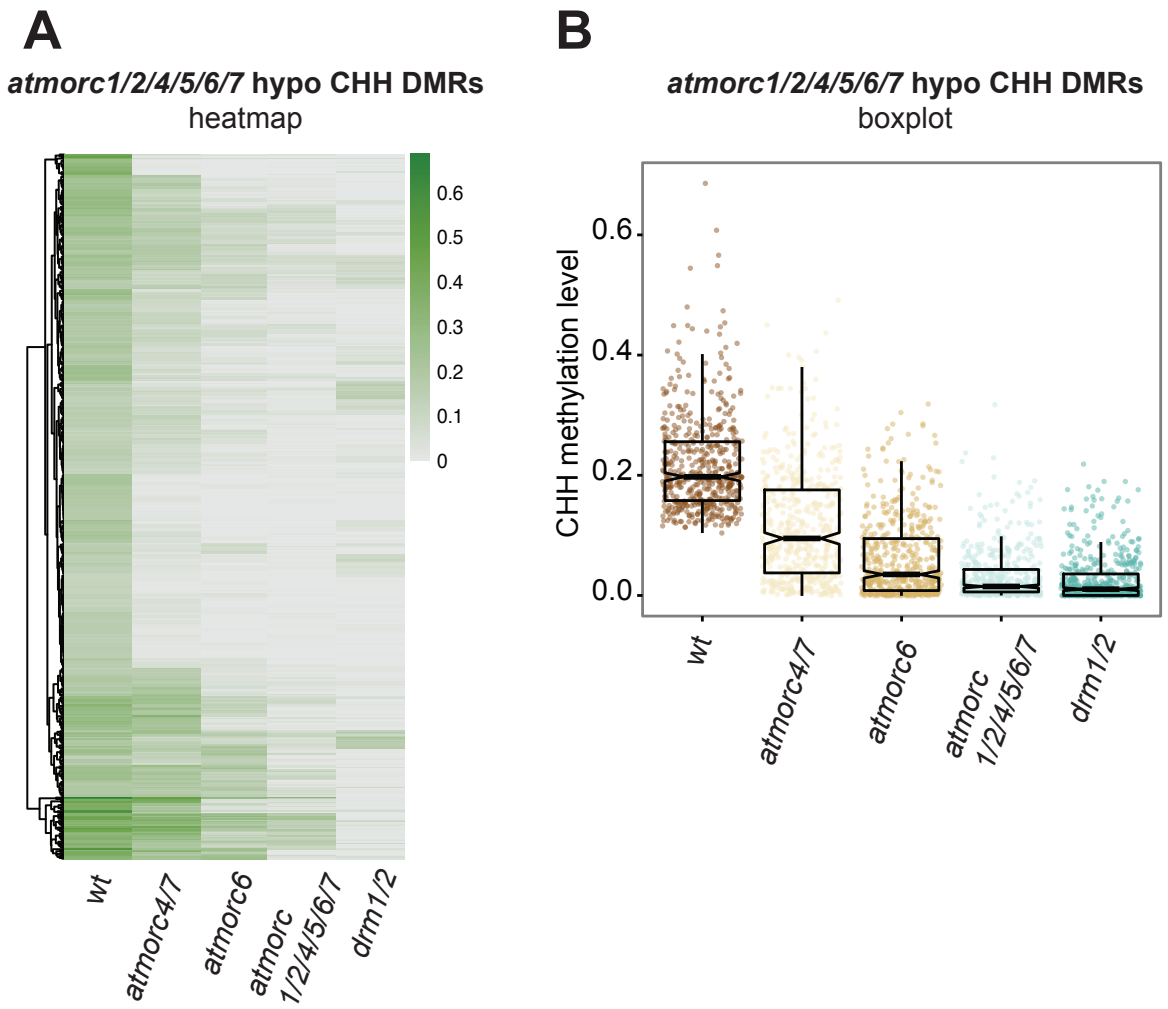

Fig. S10: *atmorc1/2/4/5/6/7* hypo CHH DMRs show evidence for transcriptional de-repression.

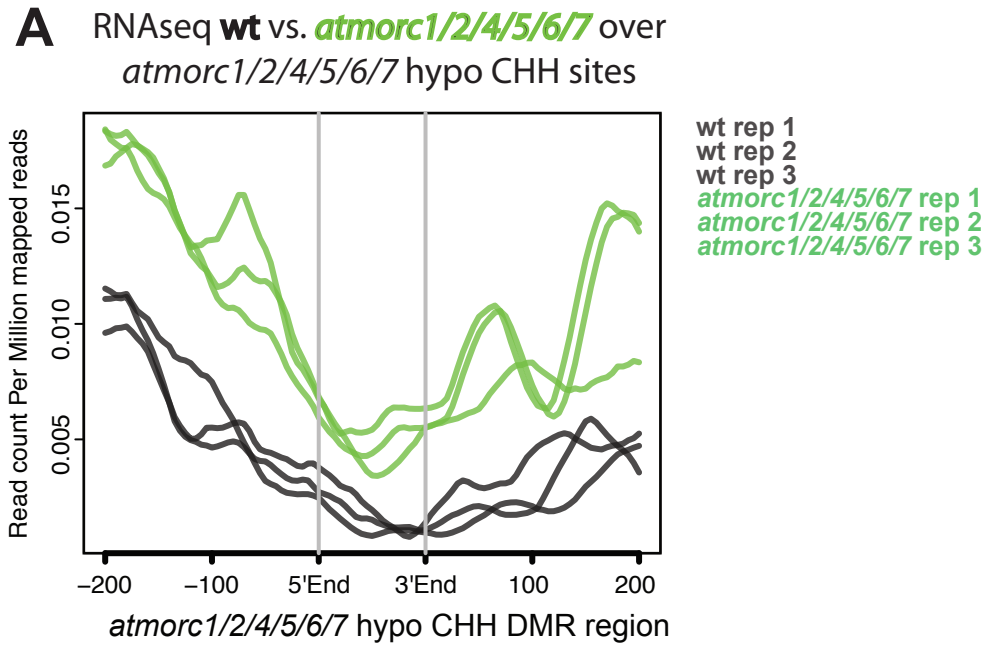

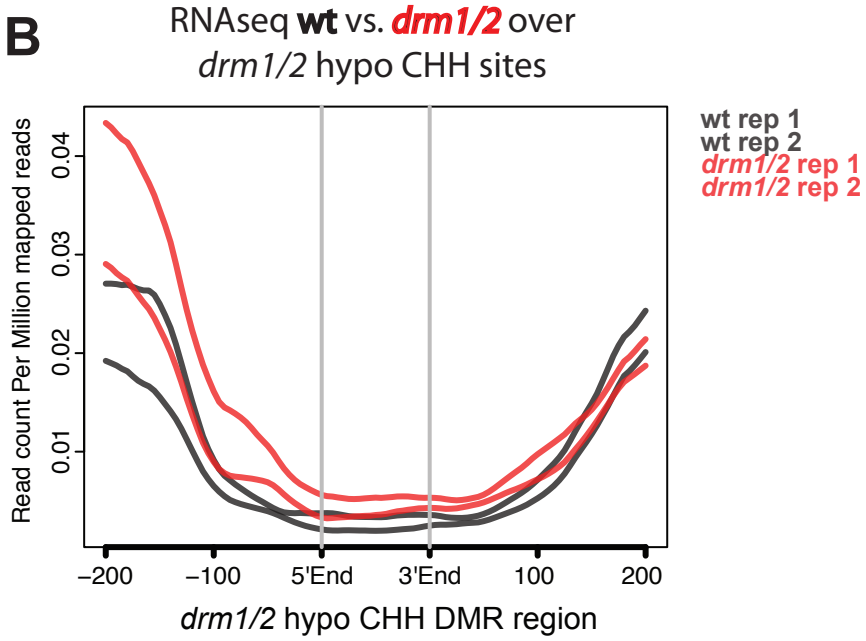

Table S1: Primers used in this study.

RT-PCR primers		
AtMu1	TAATTTGGCTGACGGAATCAC	ATTTGGGGGAAAACAAATGAG
HYPO	AACTCGGGAAAATCAGTTGCT	TTCTTCATGCCGTAAGCTGTT
SDC	AATGTAAGTTGTAAACCATTTGAACGTGACC	CAGGCATCCGTAGAACTCATGAGC
SoloLTR	AACTAACGTCATTACATACACATCTTG	AATTAGGATCTTGTTTGCCAGCTA
UNK	AAGTGGTGAGAAAGCAGAAACGAG	ACCCACTCAGCCTAACTCTACG
ROMT5	GTATCCTTTGGCCCGGTATT	GCCTCTTCGAAATGCCATAA
Actin 7	TCGTGGTGGTGAGTTTGTTAC	CAGCATCATCACAAGCATCC
morc4-1 T-DNA GK-249F08	ATGGAGCCTATCGTGAAGC	GCCACCTGCAGAAACTTCC
morc7-1 T-DNA SALK_051729	ATCCTATTCCTGCGAATCCG	CTCCATATGATTCAGACTGTGG
UBQ10	GATCTTTGCCGGAAAACAATTGGAGG	CGACTTGTCATTAGAAAGAAAGAGAT
Genotyping primers		
atmorc1-2 SAIL_893_B06	TTGCAGTTTGGAACCAAAATC	TGAGTTTTGACGACGATGATG
atmorc2-1 SALK_072774C	CTACTCAGAGCGTTGGCATTC	GTTGTAGCTGTATGGGGCTTG
atmorc3-2 SALK_043244	TTGTGTCCTAATGTGCTGTGG	AATCAAGCCATATGCAAATCC
atmorc4-1 GK-249F08	TCAGGAAAGATTTCACGAATTG	ACCTGCAGAAACTTCCCAATC
atmorc5-1 SALK_049050C	GTTGGGATAGATAAGGCGACC	TGTCGAGAAATCGTTCCTTTG
atmorc6-3 GABI_599B06	ACATCTTCCAATGGCTGAATC	GCTGGTGTCACTTCTTCATCC
atmorc7-1 SALK_051729	GTCGAAAGGATGTGAGAAACG	TTCCATTCAATTGCTTGGTTC